Control of the COVID-19 System by Vaccination Using a New Control Engineering Technique

Hazem Ibrahim Ali
Control and Systems Engineering Department, University of Technology-Iraq
Ali Hassan Mhmood (ali.h.mhmood@tu.edu.iq)
Tikrit University https://orcid.org/0000-0002-9413-7440

Research Article

Keywords: COVID-19 pandemic, Vaccination plan, SEIR epidemiological model, Control engineering, Black hole optimization

Posted Date: January 4th, 2022

DOI: https://doi.org/10.21203/rs.3.rs-1220281/v1

Control of the COVID-19 System by Vaccination Using a New Control Engineering Technique

Hazem I. Ali[1] Ali H. Mhmood[2]

Hazem.I.Ali@uotechnology.edu.iq ali.h.mhmood@tu.edu.iq

[1] Control and Systems Engineering Department, University of Technology-Iraq, Baghdad, Iraq.

[2] Department of Petroleum Systems Control Engineering, College of Petroleum Processes Engineering, Tikrit University, Iraq.

Abstract

In this work, a novel control engineering method is proposed to achieve a control strategy by vaccination for the COVID-19 epidemic. A proper mathematical model with vaccination control is developed for the COVID-19 system based on the Susceptible-Exposed-Infectious-Recovered (SEIR) epidemiological model after conducting some analyses and assumptions that reflect the COVID-19 features. Then, the proposed control law is designed using the feedback linearization approach and the H-infinity control framework. In addition, a model reference control is incorporated to ensure that satisfactory time responses are obtained. The Black Hole Optimization (BHO) technique is used to attain the optimality of the proposed control method. Following that, the reported statistics and vaccination plan of the Lombardy region of Italy are utilized to assess the effectiveness of the proposed control law. Ultimately, the simulation results illustrate that the proposed control law can effectively control the COVID-19 system and correctly perform the vaccination plan by tackling the system's nonlinearity and uncertainty and realizing elegant asymptotic tracking characteristics with reasonable control effort.

Keywords

COVID-19 pandemic, Vaccination plan, SEIR epidemiological model, Control engineering, Black hole optimization.

1. Introduction

Since the end of 2019, the planet has been witnessing an outbreak of coronavirus disease (COVID-19), which was first detected on 31 December 2019 in Wuhan, China. According to reports, the disease is caused by the severe acute respiratory syndrome coronavirus 2 (SARS-CoV-2) that can spread widely in crowded places and gatherings, where individuals devote most of their time [1]. Therefore, the virus has swiftly spread throughout the world, posing an epidemic threat and adversely affecting human social life [2].

Before the invention of vaccines, many community health techniques such as mitigation, suppression, and shield immunity have been suggested and used to control the COVID-19 outbreak [3-5]. They have been applied in many countries with different degrees of effectiveness depending on how individuals react to prescribed policies. However, the strategies mentioned above are only temporary measures that aid in slowing the outbreak's rapid expansion until vaccinations are available. Recently, several vaccines have been developed and authorized for use in many countries, such as Pfizer-BioNTech, AstraZeneca-Oxford, Moderna, and Sinopharm vaccines [6]. The governments have adopted automated systems to administer and monitor the vaccination process. In addition, various vaccination strategies to combat the COVID-19 epidemic have been studied [7-9]. Regardless of the vaccine administered, studies indicate that vaccination aims to reduce virus transmission by increasing individuals' immunity as quickly as possible.

Control engineering has played a valuable role in analyzing the COVID-19 outbreak and offering innovative solutions to tackle it [10]. Many control techniques have been designed in this sector, such as robust sliding mode control [11], nonlinear robust control based on the Lyapunov analysis [12], robust optimal model predictive feedback control [13], nonlinear robust control based on state estimation [14], and nonlinear adaptive control [15]. However, the prior control approaches were designed to implement mitigation and suppression

measures only and have treated the COVID-19 system with constant parameter values during the study period, although in reality, such values may vary from day to day. Furthermore, a variety of mathematical models has been suggested in previous studies to quantitatively describe the behavior of the COVID-19 system based on the epidemiological models [10]. The elementary version of these models is the standard Susceptible-Infectious-Recovered (SIR) model that represents the COVID-19 system using three state variables [16]. Then, due to the virus's rapid spread, the SIR model was updated to the Susceptible-Exposed-Infectious-Recovered (SEIR) version, which is characterized using four state variables [11, 12]. Moreover, the SIR model has been expanded to define the COVID-19 epidemic with more than four state variables [13, 14].

It is motivated by prior studies that modern control theory can be leveraged to design an efficient control strategy by vaccination to reduce virus transmission permanently by increasing individual immunity. Besides, robust control is the essential approach that is utilized to address the control challenges of the COVID-19 outbreak and overcome the shortcomings of the previously proposed control methods by considering system parameter fluctuations. It is also desirable to develop an optimal robust control strategy to attain better vaccination outcomes.

The contribution of this paper is to design an effective control strategy by vaccination for the COVID-19 system using a new optimal nonlinear robust control approach by addressing the system's nonlinearity and uncertainty under different variations. The conventional SEIR model is modified using COVID-19 pandemic characteristics to formulate an effective dynamical model for the COVID-19 system. In addition, the Black Hole Optimization (BHO) method is adopted to optimize the proposed control method. Lastly, the results are analyzed and discussed based on the vaccination programme of the Lombardy region of Italy.

2. Materials and Methods

In this section, the mathematical model of the COVID-19 system appropriate for vaccination control is constructed based on the mathematics of epidemiological diseases. Besides that, the proposed control strategy is presented in detail, as are the methods and algorithms utilized to complement the control design process.

2.1.COVID-19 System Mathematical Modelling

The COVID-19 system modelling process is split into two stages. The first stage is to identify an adequate epidemiological model to be customized using specific analyses and assumptions to represent the dynamical model of the COVID-19 system suited for vaccination control. Then, the second stage is to properly assign the prompt of the vaccination control input in that model. The standard SEIR model is convenient in many cases for deriving the mathematical model of the COVID-19 pandemic and is defined as follows [10-12]:

$$\begin{aligned} \dot{S}(t) &= -\frac{\beta S(t) I(t)}{N} \\ \dot{E}(t) &= \frac{\beta S(t) I(t)}{N} - \epsilon E(t) \\ \dot{I}(t) &= \epsilon E(t) - \sigma I(t) \\ \dot{R}(t) &= \sigma I(t) \end{aligned} \tag{1}$$

where N refers to the study overall population, $S(t)$ denotes the susceptible individuals, $E(t)$ stands for the exposed individuals, who have been infected but are still noninfectious, $I(t)$ indicates for the infectious individuals, and $R(t)$ signifies individuals who have acquired immunity via vaccination. Besides, the parameters β, ϵ, and σ are the virus transmission rate per unit time, the inverse of the average latent period of the disease, the inverse of the disease's average infective period, respectively. In this scenario, the population is broken down into four categories: susceptible, exposed, infectious, and immune [2]:

$$N = S(t) + E(t) + I(t) + R(t) \tag{2}$$

Hence, the population dynamic is described as:

$$\dot{N} = \dot{S}(t) + \dot{E}(t) + \dot{I}(t) + \dot{R}(t) \tag{3}$$

After that, for the SEIR model to mimic the behavior of the COVID-19 system, the following assumptions are made:

Assumption 1 When analyzing the COVID-19 pandemic, the preventive mindset requires considering the worst-case possibility. Thus, due to the rapid spread of the virus and the lengthy recovery period, it is safe to assume that the entire population is susceptible, i.e., $S(t) = N$ [10].

Assumption 2 Since the main effect of vaccination is preventive rather than curative, and the rate of infection in newborns is low, the rates of deaths and births are neglected.

Assumption 3 As new rapid testing techniques for the virus have been developed and used [17], delays during the detection and testing processes for infected cases are neglected.

Assumption 1 leads to the result that the ratio $\frac{S(t)}{N}$ equals one. Then, simply replacing this value into Eq. (1) yields:

$$\begin{aligned} \dot{S}(t) &= -\beta I(t) \\ \dot{E}(t) &= \beta I(t) - \epsilon E(t) \\ \dot{I}(t) &= \epsilon E(t) - \sigma I(t) \\ \dot{R}(t) &= \sigma I(t) \end{aligned} \tag{4}$$

Additionally, Assumption 2 indicates that the overall population is constant ($N =$ constant). Thus, the population dynamic becomes [10, 12]:

$$\dot{S}(t) + \dot{E}(t) + \dot{I}(t) + \dot{R}(t) = 0 \tag{5}$$

From the equation above, it is shown that the dynamics $\dot{S}(t)$, $\dot{E}(t)$, $\dot{I}(t)$, and $\dot{R}(t)$ are interdependent. Besides that, Eq. (5) can be manipulated to become:

$$\dot{E}(t) + \dot{I}(t) + \dot{R}(t) = -\dot{S}(t) \tag{6}$$

Hence, the property shown in Eq. (6) can be exploited to reduce the order of the SEIR model for convenience by concentrating only on the immunity, exposure, and infection dynamics. In this case, the susceptibility dynamic $\dot{S}(t)$ is removed from Eq. (4), and its behavior is monitored using Eq. (6). As a result, the SEIR model is updated to the following form:

$$\begin{aligned}\dot{R}(t) &= \sigma I(t)\\ \dot{I}(t) &= \epsilon E(t) - \sigma I(t)\\ \dot{E}(t) &= \beta I(t) - \epsilon E(t)\end{aligned} \tag{7}$$

with $\dot{S}(t) = -\dot{R}(t) - \dot{I}(t) - \dot{E}(t)$. Furthermore, Assumption 3 implies that the number of the reported and positively tested infectious cases is identical ($I_t(t) = I_r(t)$), where $I_t(t)$ and $I_r(t)$ denote the tested and reported infectious cases. It is worth noting that there is a discrepancy between actual and reported (positively tested) cases of infected individuals because many people may have no or slight symptoms and are not tested for the virus but are nonetheless infectious [10, 12]. Therefore, a variable α is introduced and utilized to convert the model in terms of formally reported cases because the data used to construct the control strategy are taken from official reports. α is defined as the ratio of reported (tested) to actual infectious cases [10], as shown below:

$$\alpha = \frac{I_r(t)}{I(t)} \tag{8}$$

Besides that, the value of α is commonly considered to be constant for a given country, but it varies considerably from one to another, ranging from about 0.02 for Germany to about 0.1 for Italy, France, and Spain [10, 12]. As a result, it is correct that:

$$\begin{aligned}R_r(t) &= \alpha R(t)\\ I_r(t) &= \alpha I(t)\\ E_r(t) &= \alpha E(t)\end{aligned} \tag{9}$$

Hence, substituting Eq. (9) in Eq. (7) gives:

$$\begin{aligned}\dot{R}_r(t) &= \sigma I_r(t)\\ \dot{I}_r(t) &= \epsilon E_r(t) - \sigma I_r(t)\\ \dot{E}_r(t) &= \beta I_r(t) - \epsilon E_r(t)\end{aligned} \tag{10}$$

with $\dot{S}_r(t) = -\dot{R}_r(t) - \dot{I}_r(t) - \dot{E}_r(t)$.

The main purpose of vaccination is to increase the immunity of individuals $R_r(t)$ while decreasing $I_r(t)$, $S_r(t)$, and $E_r(t)$. Hence, the transmission rate of the virus β is undeviatingly reduced. In this sense, β can be thought of as a

function of the vaccination control input $u(t)$ since the vaccination has a direct effect on β [10]. Moreover, the output of the model $y(t)$ is the number of individuals who have acquired immunity via vaccination $R_r(t)$. As a result, the state-space model of the COVID-19 system with vaccination control is defined as follows:

$$\begin{aligned} \dot{R}_r(t) &= \sigma I_r(t) \\ \dot{I}_r(t) &= \epsilon E_r(t) - \sigma I_r(t) \\ \dot{E}_r(t) &= \beta\big(u(t)\big) I_r(t) - \epsilon E_r(t) \\ y(t) &= R_r(t) \end{aligned} \tag{11}$$

with $\dot{S}_r(t) = -\dot{R}_r(t) - \dot{I}_r(t) - \dot{E}_r(t)$. To address the issue of disparity between actual and reported (tested) numbers of people infected, the parameters σ and ϵ are deemed uncertain with unknown upper and lower bounds in the proposed control strategy.

2.2.Black Hole Optimization (BHO) Algorithm

The BHO algorithm is an efficient black hole-inspired metaheuristic population-based optimization technique. Generally, the black hole is an area in space with a highly compressed mass into a small void. Thus, it exerts a strong gravitational pull on the nearby objects. In this instance, all matters, even light, are impotent to escape the gravity of the black hole, and they would disappear from existence [18, 19].

Because it is a population-based method, the BHO is initialized by generating an initial population of candidate solutions and defining a suitable objective function for the optimization issue. The candidates are spread haphazardly in the search space of the optimization problem of dimension d. In fact, d denotes the number of parameters that are optimized. After initialization, the following steps for every iteration outline the BHO procedure, as shown in Fig. 1 [18, 19]:

(a) The best candidate with the lower cost is identified as the black hole, while the rest represent the regular stars.

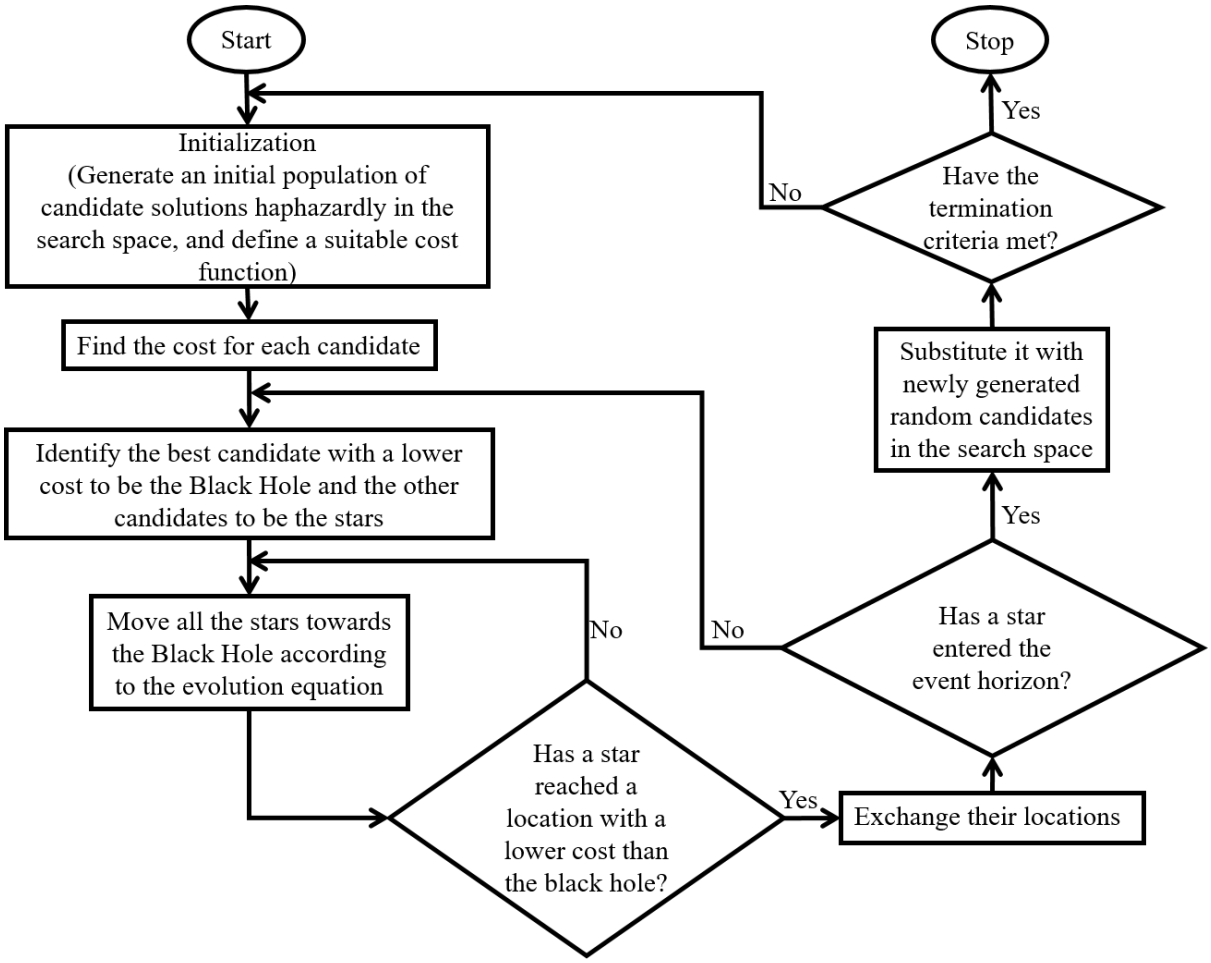

Fig. 1. The BHO algorithm flowchart.

(b) Then, the population is evolved by directing the stars towards the black hole based on the evolution equation below:

$$x_i(t+1) = x_i(t) + rand \times \left(x_{BH} - x_i(t)\right); \quad i = 1, 2, \dots, n \tag{12}$$

where $x_i(t+1)$ and $x_i(t)$ are the ith star locations at iterations $(t+1)$ and (t), respectively, x_{BH} is the location of the black hole, $rand$ is a random real number between 0 and 1, and n is the number of the stars.

(c) While its motion, a star may attain a lower-cost location than the black hole. In this situation, the black hole is updated by identifying that star as a new black hole. Afterward, the BHO method progresses with that new black hole, and the other stars move towards it.

(d) When a star gets in the black hole scope termed as the event horizon, it is devoured by the black hole and supplanted with a new candidate generated at random in the search space. The following is the radius of the event horizon:

$$R = \frac{f_{BH}}{\sum_{i=1}^{N} f_i} \tag{13}$$

where f_{BH} and f_i are the cost values of the black hole and ith star, respectively.

(e) Eventually, the BHO procedure is terminated when either a desirable cost or the maximum number of iterations are attained. The best costs would be identical after many iterations, indicating that there are no more best solutions.

The BHO algorithm has two considerable advantages. Firstly, it has a straightforward framework that makes it simpler to formulate. Secondly, it is devoid of parameter tuning perplexities [18, 19].

2.3. Optimal Nonlinear robust Controller Design

In this subsection, the proposed controller is designed to achieve a control strategy by vaccination for the COVID-19 pandemic, whose dynamics are described in Eq. (11). The design method of the proposed controller is conducted using the feedback linearization approach and the H-infinity control framework. Besides that, the proposed controller is induced to accomplish a desirable time response using the model reference control scheme, where a decent reference model is defined, and its performance is enforced as a reference response on the closed-loop system. The proposed controller's duties are to compensate the nonlinearity and uncertainty of the COVID-19 system with adequate robustness and obtain proper asymptotic tracking properties between the system states ($R_r(t)$, $I_r(t)$, and $E_r(t)$) and the reference model states.

Primarily, Eq. (11) shows that the system has mismatched perturbations in the two upper subsystems ($\dot{R}_r(t)$ and $\dot{I}_r(t)$). Such perturbations cannot be directly compensated by the control input unless the system model is rewritten in

an equivalent controllable structure, where the matching conditions are relaxed, and the nonlinearity and uncertainty (system perturbations) appear in the same subsystem channel of $\beta\big(u(t)\big)$ [18-20]. Thus, a state variable transformation is applied using the following diffeomorphism mapping [12, 18-20]:

$$z(t) = T\left(\begin{bmatrix} R_r(t) \\ I_r(t) \\ E_r(t) \end{bmatrix}\right) \tag{14}$$

where $T(.)$ refers to the transformation operator. The mapping is then performed as follows:

$$\begin{aligned} z_1(t) &= R_r(t) \\ z_2(t) &= \dot{z}_1(t) = \dot{R}_r(t) \\ z_3(t) &= \dot{z}_2(t) = \ddot{z}_1(t) = \ddot{R}_r(t) \end{aligned} \tag{15}$$

As a result, the COVID-19 system dynamics in terms of $z(t)$ become as follows:

$$\begin{aligned} \dot{z}_1(t) &= z_2(t) \\ \dot{z}_2(t) &= z_3(t) \\ \dot{z}_3(t) &= -\epsilon\sigma z_2(t) - (\epsilon + \sigma) z_3(t) + \epsilon z_2(t)\beta\big(u(t)\big) \\ y(t) &= z_1(t) \end{aligned} \tag{16}$$

The system model can also be expressed in matrix notation in the following form:

$$\begin{aligned} \dot{z}(t) &= Az(t) + Bz_2(t)\beta\big(u(t)\big) \\ y(t) &= Cz(t) \end{aligned} \tag{17}$$

where:

$$A = \begin{bmatrix} 0 & 1 & 0 \\ 0 & 0 & 1 \\ 0 & -\epsilon\sigma & -(\epsilon + \sigma) \end{bmatrix},\ z(t) = \begin{bmatrix} z_1(t) \\ z_2(t) \\ z_3(t) \end{bmatrix},\ B = \begin{bmatrix} 0 \\ 0 \\ \epsilon \end{bmatrix},\ \text{and } C = [1 \quad 0 \quad 0] \tag{18}$$

It is noteworthy that the proposed control law is made up of two parts: nonlinear and robust. The nonlinear component is designed to compensate the system's nonlinearity using the feedback linearization method. In this sense, an exact linearization is realized, and the uncertain nonlinear dynamics of the system are algebraically converted to a corresponding uncertain linear model. After that, the robust part is developed to address the uncertainty of the system [20]. Hence, let:

$$\beta\big(u(t)\big) = \frac{1}{z_2(t)}\beta_{AUX}\big(u(t)\big) \tag{19}$$

where $\beta_{AUX}\big(u(t)\big)$ is an auxiliary component of the control law. Then, inserting Eq. (19) in Eq. (17) results in:

$$\begin{aligned} \dot{z}(t) &= Az(t) + B\beta_{AUX}\big(u(t)\big) \\ y(t) &= Cz(t) \end{aligned} \tag{20}$$

where the matrices A and B are unknown, including two uncertain parameters ϵ and σ. The uncertainties in ϵ and σ arise due to variations in their real values from the reported (nominal) ones since there is a probable disparity between the actual and reported (tested) numbers of infected people. Therefore, the robust part of the control law is designed using an efficient robust control approach that is the H-infinity state feedback control [20], where the parametric uncertainties are first extracted from the system's nominal model and a customized term is formed for them, then their input is treated as an exogenous signal. The uncertain parameters ϵ and σ are described as follows [18-20]:

$$\epsilon = \epsilon_r + \delta_\epsilon \tag{21}$$

$$\sigma = \sigma_r + \delta_\sigma \tag{22}$$

where δ_ϵ and δ_σ denote the variations in ϵ and σ from the reported values ϵ_r and σ_r, respectively. Consequently, using Eqs. (21) and (22), the system uncertainties are extracted, and the system dynamics take the following form:

$$\begin{aligned} \dot{z}(t) &= A_r z(t) + B_1 w_a(t, z, u) + B_r \beta_{AUX}\big(u(t)\big) \\ y(t) &= Cz(t) \end{aligned} \tag{23}$$

where $w_a(t, z, u) = -\delta_{\epsilon\sigma} z_2(t) - \delta_{(\epsilon+\sigma)} z_3(t) + \delta_\epsilon \beta_{AUX}\big(u(t)\big)$ represents the uncertainty input. In addition:

$$A_r = \begin{bmatrix} 0 & 1 & 0 \\ 0 & 0 & 1 \\ 0 & -\epsilon_r\sigma_r & -(\epsilon_r + \sigma_r) \end{bmatrix},\ B_1 = \begin{bmatrix} 0 \\ 0 \\ 1 \end{bmatrix},\ \text{and } B_r = \begin{bmatrix} 0 \\ 0 \\ \epsilon_r \end{bmatrix} \tag{24}$$

Then, as the system is third-order, the following globally asymptotically stable system model is adopted as a reference model [20]:

$$\dot{z}_d(t) = A_d z_d(t) + B_d r(t)$$
$$y_d(t) = C z_d(t) \quad (25)$$

where $z_d(t)$, $r(t)$, and $y_d(t)$ represent the reference model states, vaccination command input, and reference model output, respectively. Moreover [21]:

$$z_d(t) = \begin{bmatrix} z_{d1}(t) \\ z_{d2}(t) \\ z_{d3}(t) \end{bmatrix}, A_d = \begin{bmatrix} 0 & 1 & 0 \\ 0 & 0 & 1 \\ -\omega_n^3 & -2.15\omega_n^2 & -1.75\omega_n \end{bmatrix}, \text{and } B_d = \begin{bmatrix} 0 \\ 0 \\ \omega_n^3 \end{bmatrix} \quad (26)$$

where ω_n denotes the natural frequency of the reference model. It is appropriately manipulated to develop a proper time response. The asymptotic tracking duty involves the design of a control law that meets the following criterion [18-20]:

$$\lim_{t\to\infty} \|e(t)\|_2 = 0 \quad (27)$$

where $e(t)$ stands for the tracking error vector defined as the difference between the system and reference model states:

$$e(t) = z(t) - z_d(t) \quad (28)$$

The time derivative of Eq. (28) gives:

$$\dot{e}(t) = \dot{z}(t) - \dot{z}_d(t) \quad (29)$$

Substituting Eqs. (23) and (25) in Eq. (29) yields:

$$\dot{e}(t) = A_r z(t) + B_1 w_a(t, e, u) + B_r \beta_{AUX}\big(u(t)\big) - A_d z_d(t) - B_d r(t) \quad (30)$$

Adding $\big(A_r z_d(t) - A_r z_d(t)\big)$ to Eq. (30) renders the tracking error dynamics of the COVID-19 system shown below:

$$\dot{e}(t) = \begin{pmatrix} A_r z(t) + B_1 w_a(t, e, u) + \\ B_r \beta_{AUX}\big(u(t)\big) \end{pmatrix} - A_d z_d(t) - B_d r(t) + \begin{pmatrix} A_r z_d(t) - \\ A_r z_d(t) \end{pmatrix} \Longrightarrow$$

$$\dot{e}(t) = \begin{pmatrix} A_r e(t) + B_1 w_a(t, e, u) + \\ B_r \beta_{AUX}\big(u(t)\big) \end{pmatrix} + (A_r - A_d) z_d(t) - B_d r(t) \quad (31)$$

Afterward, by letting:

$$\beta_{AUX}\big(u(t)\big) = \frac{1}{\epsilon_r} \begin{pmatrix} \omega_n^3 r(t) - \omega_n^3 z_{d1}(t) + \\ (\epsilon_r \sigma_r - 2.15\omega_n^2) z_{d2}(t) + \\ \big((\epsilon_r + \sigma_r) - 1.75\omega_n\big) z_{d3}(t) \end{pmatrix} + \beta_R\big(u(t)\big) \quad (32)$$

where $\beta_R\big(u(t)\big)$ is the control input of the control law's robust component, the tracking error dynamics take the form of the H-infinity state feedback control problem, as shown below:

$$\begin{aligned}\dot{e}(t) &= A_r e(t) + B_1 w_a(t,e,u) + B_r \beta_R\big(u(t)\big)\\ h(t) &= C_1 e(t) + D_{12}\beta_R\big(u(t)\big)\\ y_e(t) &= Ce(t)\end{aligned} \tag{33}$$

where $y_e(t)$ is the system output in terms of the tracking error dynamics, and $h(t)$ is a penalty vector of uncertainty-affected outputs whose magnitudes should be controlled pursuant to weights prescribed by the matrices C_1 and D_{12}.

Assumption 4 It is assumed in designing $\beta_R\big(u(t)\big)$ that [18, 20]:

1) The pairs (A_r, B_1) and (A_r, B_r) are controllable or leastwise stabilizable.
2) The pair (C_1, A_r) is observable or leastwise detectable.
3) $C_1^T D_{12} = \mathbf{0}$ and $D_{12}^T D_{12} = \varepsilon I$.

Thus, the matrices C_1 and D_{12} are formulated as follows:

$$C_1 = \begin{bmatrix} c_{11} & c_{12} & c_{13} \\ c_{21} & c_{22} & c_{23} \\ c_{31} & c_{32} & c_{33} \\ 0 & 0 & 0 \end{bmatrix} \tag{34}$$

$$D_{12} = \begin{bmatrix} 0 \\ 0 \\ 0 \\ \sqrt{\varepsilon} \end{bmatrix} \tag{35}$$

where ε denotes a weight related to the magnitude of $\beta_R\big(u(t)\big)$. Moreover, the H-infinity state feedback control law is expressed in the form [20]:

$$\beta_R\big(u(t)\big) = K_{\beta_R} e(t) \tag{36}$$

where K_{β_R} is the gain matrix of $\beta_R\big(u(t)\big)$. The attractive feature of the proposed control strategy is manifested in assuming that ϵ and σ are bounded, with known reported (nominal) values and unknown upper and lower bounds. Thus, the uncertainty input $w_a(t,e,u)$ is treated in terms of its worst-case scenario, which is defined as follows [20]:

$$w_a(t,e,u) = K_{w_a} e(t) \tag{37}$$

where K_{w_a} is the gain matrix of the worst-case uncertainty. Then, substituting Eqs. (36) and (37) in Eq. (33) gives the following closed-loop tracking error dynamics:

$$\begin{aligned} \dot{e}(t) &= \left(A_r + B_1 K_{w_a} + B_r K_{\beta_R}\right) e(t) \\ h(t) &= \left(C_1 + D_{12} K_{\beta_R}\right) e(t) \\ y_e(t) &= C e(t) \end{aligned} \tag{38}$$

The H-infinity control problem is defined as the design of a state feedback control law of Eq. (36) that minimizes the infinity norm of the closed-loop transfer function matrix $G_{hw_a}(s)$ from $w_a(t,e,u)$ to $h(t)$ to be less than or equal to γ [18]:

$$\left\| G_{hw_a}(s) \right\|_\infty \leq \gamma \tag{39}$$

where γ is a real positive number that represents the system's robustness factor. The requirement of Eq. (39) intimates that the cost function given below can be adopted for the robustness issue [18, 20]:

$$J(\beta_R, w_a) = \int_0^\infty (h^T h - \gamma^2 w_a^T w_a) dt \tag{40}$$

Using Assumption 4 and Eqs. (37) and (38), it is determined that:

$$J(\beta_R, w_a) = \int_0^\infty \left(e^T \left[C_1^T C_1 + \varepsilon K_{\beta_R}^T K_{\beta_R} - \gamma^2 K_{w_a}^T K_{w_a}\right] e\right) dt \tag{41}$$

Then, a Lyapunov function candidate for the proposed control method is defined in the following form [18, 20]:

$$V(e) = e^T P e \tag{42}$$

where P is a real symmetric positive definite matrix. Besides, the time derivative of $V(e)$ is computed as follows:

$$\dot{V}(e) = e^T P \dot{e} + \dot{e}^T P e \tag{43}$$

Substituting Eq. (38) in Eq. (43) yields:

$$\dot{V}(e) = e^T \left[P\left(A_r + B_1 K_{w_a} + B_r K_{\beta_R}\right) + \left(A_r + B_1 K_{w_a} + B_r K_{\beta_R}\right)^T P\right] e \tag{44}$$

Afterward, by setting [18, 20]:

$$-\dot{V}(e) = e^T\left[C_1^T C_1 + \varepsilon K_{\beta_R}^T K_{\beta_R} - \gamma^2 K_{w_a}^T K_{w_a}\right]e \quad (45)$$

the following equation is obtained:

$$\left[P\begin{pmatrix}A_r + B_1 K_{w_a} + \\ B_r K_{\beta_R}\end{pmatrix} + \begin{pmatrix}A_r + B_1 K_{w_a} + \\ B_r K_{\beta_R}\end{pmatrix}^T P\right] + \begin{pmatrix}C_1^T C_1 + \varepsilon K_{\beta_R}^T K_{\beta_R} - \\ \gamma^2 K_{w_a}^T K_{w_a}\end{pmatrix} = 0 \quad (46)$$

Then, differentiating Eq. (46) for K_{β_R} by taking $\frac{\partial P}{\partial K_{\beta_R}} = 0$ results in [18]:

$$K_{\beta_R} = -\varepsilon^{-1} B_r^T P \quad (47)$$

In addition, Eq. (46) is differentiated for K_{w_a} by taking $\frac{\partial P}{\partial K_{w_a}} = 0$, and K_{w_a} is gained as follows [18]:

$$K_{w_a} = \gamma^{-2} B_1^T P \quad (48)$$

Next, Eqs. (47) and (48) are inserted in Eq. (46). As a result, the following Riccati equation is formed:

$$PA_r + A_r^T P - P[\varepsilon^{-1} B_r B_r^T - \gamma^{-2} B_1 B_1^T]P + C_1^T C_1 = 0 \quad (49)$$

where the matrix P represents its unique solution. As Eq. (49) is dependent on the robustness criterion (39), the presence of its positive definite solution P suffices to meet that requirement.

The design method is optimized using the BHO method to find the minimum γ, for which $\left\|G_{hw_a}(s)\right\|_\infty$ is minimized, the optimal value of ε, and the optimal entries of the matrix C_1, with the optimization cost function:

$$J_{BHO}(\gamma, \varepsilon, C_1) = \left\|G_{hw_a}(s)\right\|_\infty \quad (50)$$

In this case, the design problem is tackled backward by implementing the BHO algorithm, solving Eq. (49), and obtaining the optimal robust controller $\beta_R\big(u(t)\big)$ using the solution P. Finally, the overall vaccination control law becomes:

$$\beta\big(u(t)\big) = \frac{1}{z_2(t)}\left(\frac{1}{\epsilon_r}\begin{pmatrix}\omega_n^3 r(t) - \omega_n^3 z_{d1}(t) + \\ (\epsilon_r\sigma_r - 2.15\omega_n^2) z_{d2}(t) + \\ \big((\epsilon_r + \sigma_r) - 1.75\omega_n\big) z_{d3}(t)\end{pmatrix} + K_{\beta_R} e(t)\right) \quad (51)$$

where K_{β_R} is defined in Eq. (47).

3. Results

The effectiveness of the proposed control law in implementing a vaccination strategy to control the COVID-19 epidemic is evaluated in this section. The results are analyzed via simulation using Matlab/Simulink software regarding the reported (nominal) values of the system parameters $\epsilon_r = 0.2\ day^{-1}$ and $\sigma_r = 0.2\ day^{-1}$ and their variations. The reported values are based on statistics of the COVID-19 outbreak in Lombardy, Italy, from February 23, 2020, to March 16, 2020, when the virus outbreak was at its peak [22]. At first, Fig. 2 shows the open-loop time response of the COVID-19 system (without control) described by the state trajectories of the immunized, infectious, and exposed individuals. It is demonstrated that the system is inherently unstable, and the virus spreads rapidly, causing a significant increase in the number of disease-infected people. Consequently, an effective control strategy by vaccination is required to control and stabilize the COVID-19 outbreak perpetually. The vaccination schedule is drawn up based on the protocol adopted by the Italian Ministry of Health to achieve immunity for leastwise 70% of the total population of Lombardy; hence, $6.6\ million$ people are planned to be vaccinated at a rate of about 170000 persons per day [23]. In this case, society develops herd immunity [24], in which two of every three persons become immune to the disease, and infection rates gradually drop to zero by increasing individual immunity. Thus, the vaccination command input is formatted as shown in Fig. 3.

By applying the BHO algorithm for (400) iterations to the tracking error dynamics exhibited in Eq. (33) along with the specified reported rates, the optimal values of the design variables γ, ε, and C_1 are determined as follows:

$$\gamma = 0.6207,\ \varepsilon = 0.0050,\ \text{and}\ C_1 = \begin{bmatrix} 3.0381 & 7.2204 & 7.1474 \\ 4.3491 & 7.9234 & 6.2379 \\ 5.9375 & 4.3601 & 3.5643 \\ 0 & 0 & 0 \end{bmatrix} \tag{52}$$

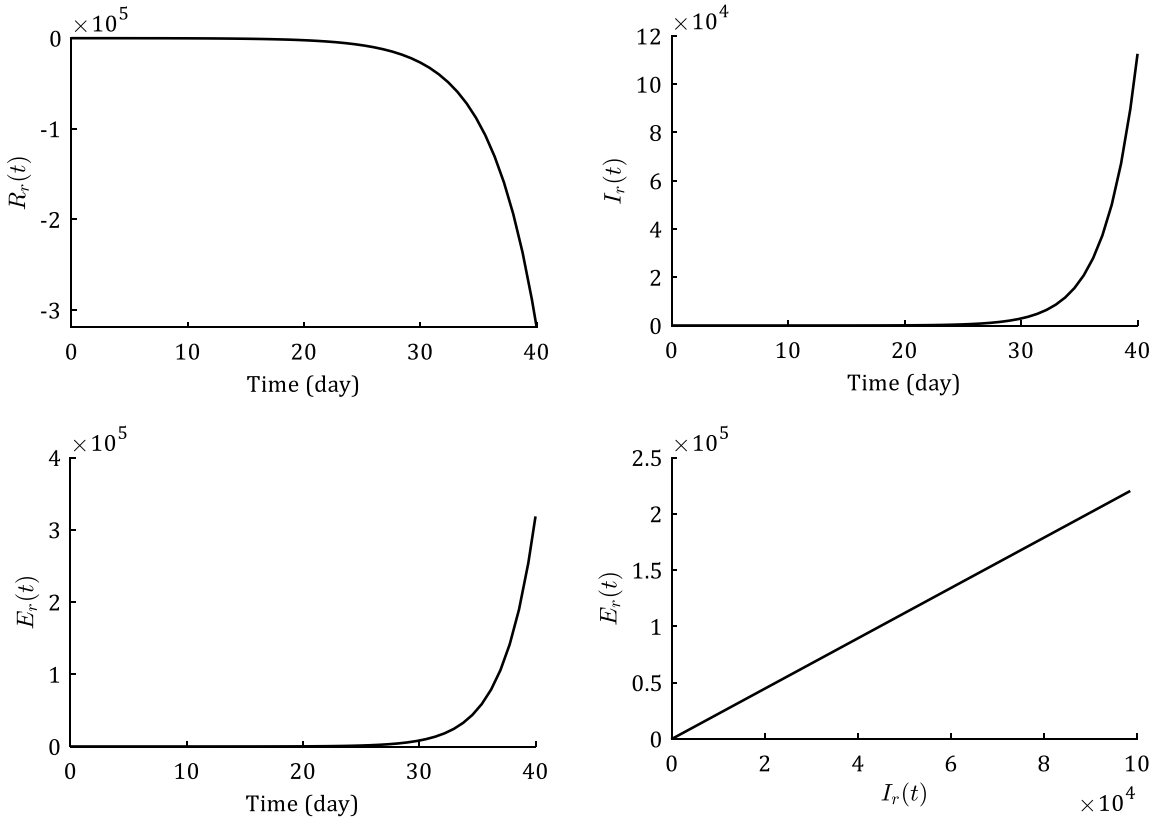

Fig. 2. Open-loop time response of the COVID-19 system (without control).

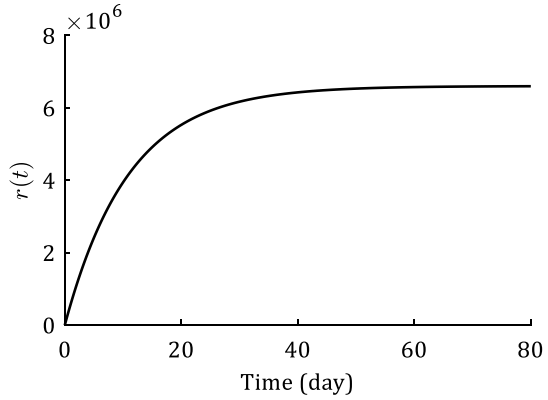

Fig. 3. Command input of the vaccination plan.

Next, Eq. (49) is solved using the previously determined values, producing the following positive definite solution:

$$P = \begin{bmatrix} 19.6009 & 14.9047 & 3.4250 \\ 14.9047 & 16.4561 & 5.4968 \\ 3.4250 & 5.4968 & 4.5132 \end{bmatrix} \tag{53}$$

As a result, the gain matrix K_{β_R} is obtained using Eq. (47) as follows:

$$K_{\beta_R} = [-137.0017 \quad -219.8729 \quad -180.5295] \tag{54}$$

Then, the vaccination control law of Eq. (51) is applied with $\omega_n = 50\, rad/day$ to the basic COVID-19 system given in Eq. (11).

Fig. 4 depicts the output characteristics of the nominal closed-loop system after applying the control law, illustrating the trajectory of the vaccinated individuals in effectively tracking the trajectories of the reference model output and vaccination command input. Additionally, the behavior and tracking features of the infectious and exposed state trajectories are exhibited in Figs. 5 and 6, respectively. It is revealed that the number of immunized individuals has increased following the vaccination plan, while the number of infectious and exposed people has reduced as predicted due to the increase in the individuals' immunity. Hence, the controlled COVID-19 system has attained nominal stability and performance attributes with proper asymptotic tracking to the reference model states despite the system's nonlinearity.

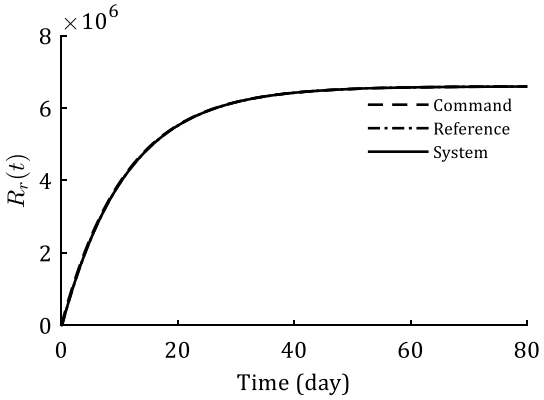

Fig. 4. Output characteristics of the nominal closed-loop system after applying the control law.

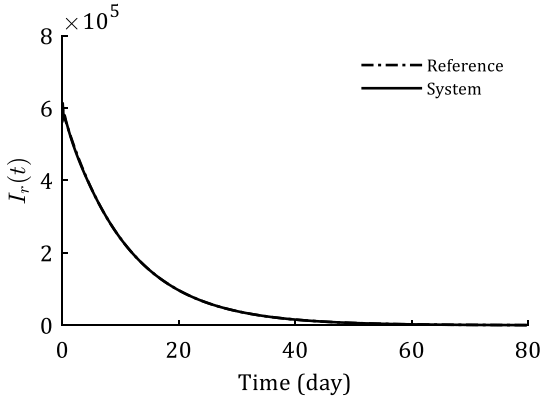

Fig. 5. State trajectory of the infectious individuals.

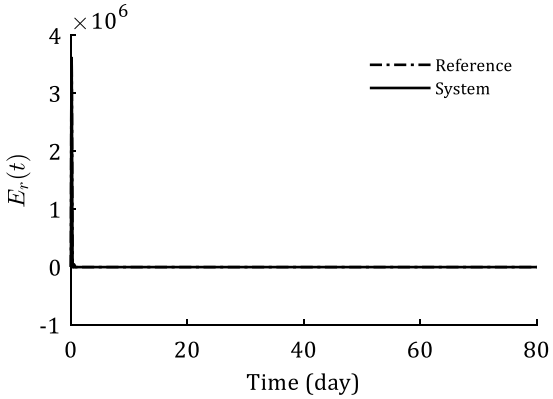

Fig. 6. State trajectory of the exposed individuals.

Fig. 7 shows the convergence of the tracking error norm to zero as time increases, confirming the achievement of the asymptotic tracking property between the system and reference model states as specified in Eq. (27). Besides, the vaccination control input is described in Fig. 8. It is shown that the magnitude of the control input is suitable compared to the high number of people vaccinated.

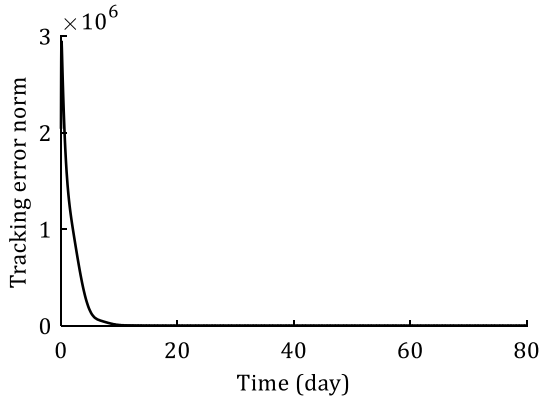

Fig. 7. Convergence of the tracking error norm.

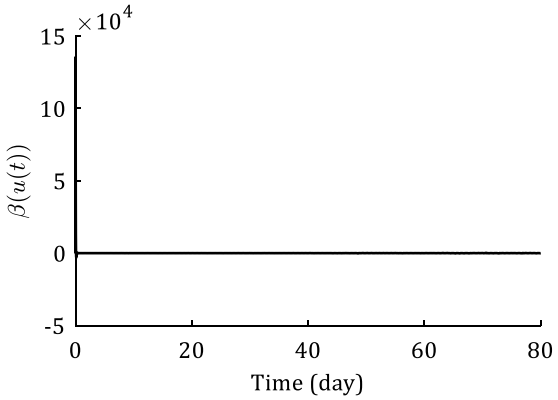

Fig. 8. Vaccination control input.

As mentioned earlier, the ratio α is estimated to be about 0.1 for Italy. Therefore, $\pm 10\%$ variations from the reported values of the system uncertain parameters ϵ and σ are considered to investigate the efficacy of the proposed control strategy against variations between reported and actual infected cases. Then, the state trajectories of the controlled uncertain COVID-19 system are illustrated in Fig. 9, asserting that the system's robust stability and performance characteristics have been achieved despite the system perturbations (nonlinearity and fluctuations in the uncertain parameters).

Figs. 10 and 11 depict the behaviors of the Lyapunov function and its time derivative. It is clear from these two figures that $V(e)$ and $\dot{V}(e)$ are positive and negative definite functions, implying that the origin point $e = \mathbf{0}$ is asymptotically stable in the face of the system's nonlinearity and uncertainty. Moreover, since the Lyapunov function is in quadratic form, it is radially unbounded, signifying that $V(e) \to \infty$ as $\|e\|_2 \to \infty$. Thus, the stability property of the origin point has

been maintained for all the state-space regions of the system, and $e = \mathbf{0}$ is globally asymptotically stable even in the presence of system perturbations.

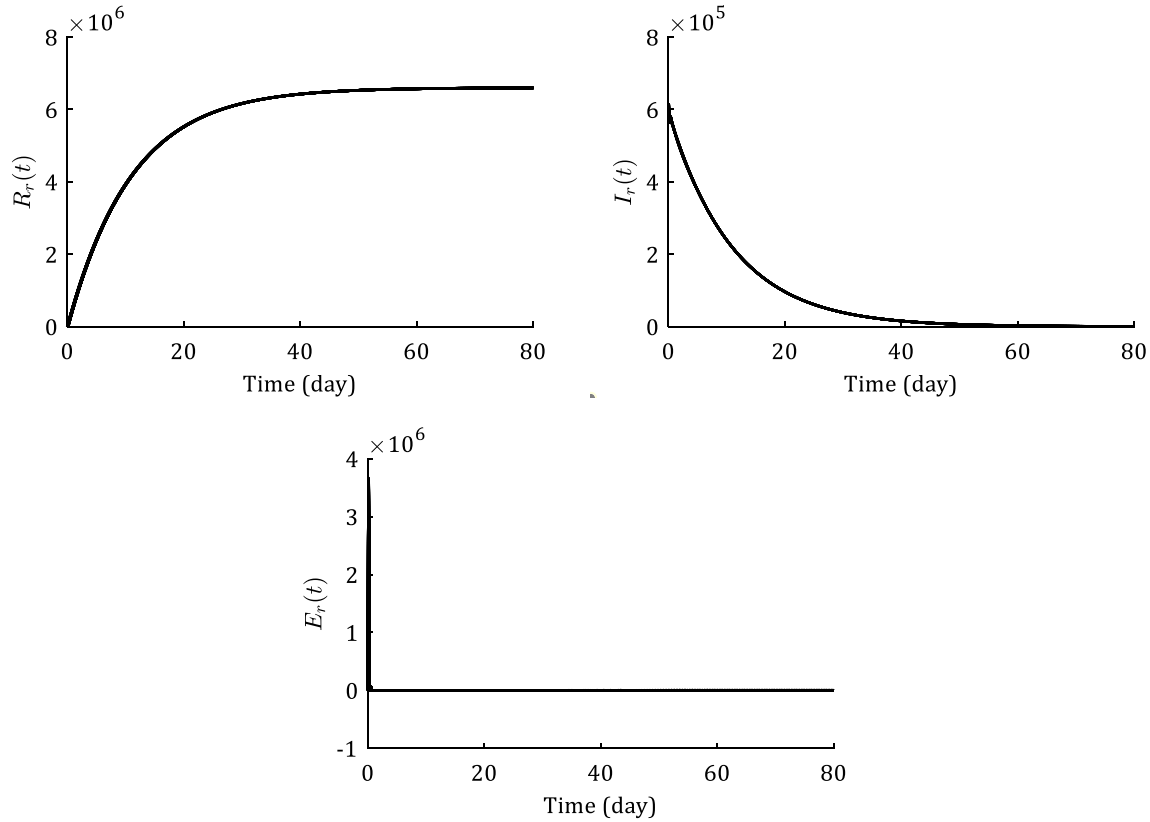

Fig. 9. State trajectories of the controlled uncertain COVID-19 system.

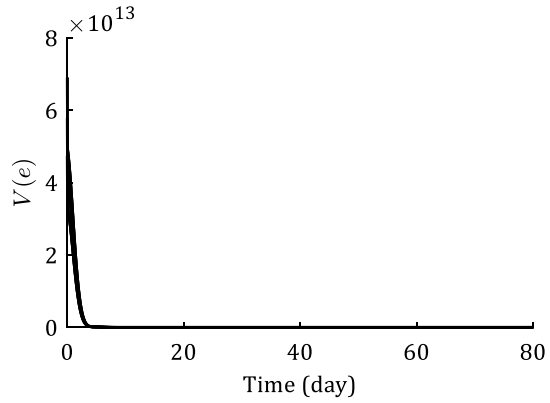

Fig. 10. Behavior of the Lyapunov function.

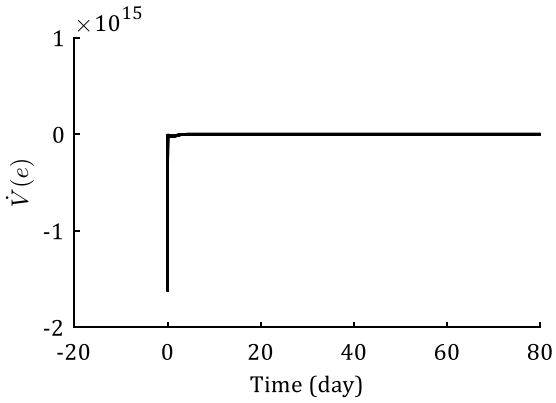

Fig. 11. Lyapunov function time derivative.

Furthermore, the phase-plane in terms of the tracking error dynamics after applying the control law is displayed in Fig. 12. It is clear that the tracking error trajectories have approached the origin point $e = \mathbf{0}$ for all changes in the uncertain parameters. As a result, the global asymptotic tracking property for the

COVID-19 system states to approach the steady-state point ($R_r(\infty) = 6.6 \times 10^6$, $I_r(\infty) = 0$, and $E_r(\infty) = 0$) have been accomplished, as shown in Fig. 13.

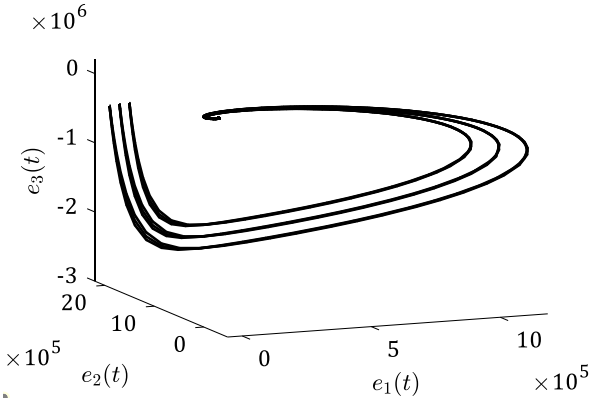

Fig. 12. Phase-plane of the tracking error dynamics.

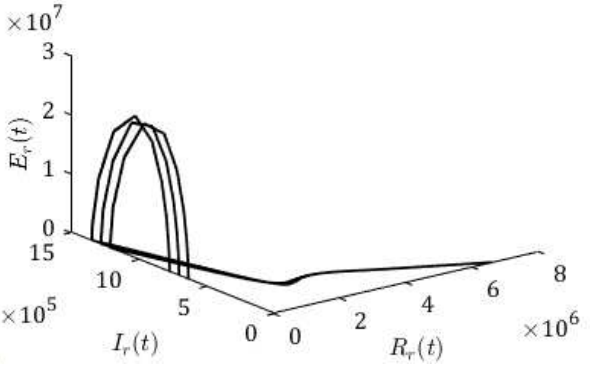

Fig. 13. Phase-plane of the controlled uncertain system.

Interestingly, it has been obtained that:

$$\left\|G_{hw_a}(s)\right\|_\infty = 0.4607 \tag{55}$$

Thus, the robustness requirement presented in equation (39) has been realized as the value of $\left\|G_{hw_a}(s)\right\|_\infty$ was smaller than γ. As a result, the proposed control method has achieved desirable robustness to the COVID-19 system, leading to uniformly bounded closed-loop signals.

The former results demonstrate that the proposed control approach has effectively controlled the COVID-19 pandemic and reduced viral transmission rates by increasing individual immunity via vaccination in a reasonable period. Besides, the designed control law has correctly executed the vaccination strategy with impactful and feasible control action, realizing interesting nominal and robust stability characteristics for the COVID-19 system. The perturbations were efficiently compensated with substantial robustness, and adequate time responses were attained by achieving exact asymptotic tracking performance to a globally asymptotically stable reference model. It is worth mentioning that as the value of γ becomes low, the control approach can compensate higher variations between

reported and actual infected cases. However, it should be assured that the values of γ always exhibit the necessary inequality:

$$\varepsilon^{-1}B_r B_r^T - \gamma^{-2}B_1 B_1^T \geq \mathbf{0} \quad (56)$$

Anything else, the solution matrix P would not be positive definite, and the design would be considered a failure. Finally, the paper strategy is compared to the work presented in [12], which proposed a robust nonlinear control algorithm to control the COVID-19 system. Although the work was interesting, it had the following flaws:

1) The strategy involved interim mitigation and suppression efforts for a specific period.
2) The COVID-19 system model was developed using the SEIR paradigm, with a focus on two state variables only.
3) The control law had a discontinuity property related to the signum function $sign(.)$, causing unwanted chattering in the system signals.
4) The control input initially had a high magnitude of 12×10^6 and 8×10^6, while the highest output achieved was about 4500 people. This issue negatively influences the feasibility of the control approach.

On the other side, this work represents a definitive solution to the COVID-19 outbreak based on a vaccination process. Additionally, the COVID-19 system model has been derived with three direct state variables and a fourth indirect one. This feature proved effective in providing better knowledge about the system's behavior. Furthermore, the proposed control law was of the continuous kind, applying a reasonable initial control effort, as shown in Fig. 8.

4. Conclusion

In this paper, a novel vaccination control law has been designed for the COVID-19 system. It was made up of nonlinear and robust components. The nonlinear part has been constructed based on the feedback linearization method to compensate the system nonlinearity, while the robust part was developed using

the H-infinity control framework to address the system uncertainty. Certain analyses and assumptions based on the COVID-19 properties were applied to the SEIR epidemiological model to derive a decent mathematical model with vaccination control for the COVID-19 system. Besides, the system parameters have been assumed to be uncertain with bounded variations, but the variation percentages are not required to be known. The design approach's optimality has been attained by designing the control law against worst-case uncertainty and applying the BHO method to determine the optimal design parameters. Furthermore, the results obtained show that the control approach has controlled the COVID-19 outbreak in Lombardy, Italy, during a satisfactory duration with more desirable stability and performance qualities. Finally, the proposed control method by vaccination can be used for additional regions at any time.

CRediT authorship contribution statement

Hazem I. Ali: Conceptualization, Methodology, Visualization, Formal analysis, Supervision, Investigation, Writing – review and editing. **Ali H. Mhmood:** Methodology, Software, Data curation, Writing- Original draft preparation.

Declaration of Competing Interest

The authors declare that they have no known competing financial interests or personal relationships that could have appeared to influence the work reported in this paper.

Data Availability Statements

Data sharing is not applicable to this article as no datasets were generated or analyzed during the current study.

References

[1] World Health Organization, Coronavirus disease (COVID-19) situation reports, 2020 (accessed 29 November 2021), https://www.who.int/emergencies/diseases/novel-coronavirus-2019/situation-reports.

[2] H. A. Rad, A. Badi, A study on control of novel corona-virus (2019-nCoV) disease process by using PID controller, MedRxiv (2020). https://doi.org/10.1101/2020.04.19.20071654.

[3] P. Yang, J. Qi, S. Zhang, X. Wang, G. Bi, Y. Yang, B. Sheng, G. Yang, Feasibility study of mitigation and suppression strategies for controlling COVID-19 outbreaks in London and Wuhan, PloS ONE 15 (2020) e0236857. https://doi.org/10.1371/journal.pone.0236857.

[4] H. Sjödin, A. F. Johansson, Å. Brännström, Z. Farooq, H. K. Kriit, A. Wilder-Smith, C. Åström, J. Thunberg, M. Söderquist, J. Rocklöv, COVID-19 healthcare demand and mortality in Sweden in response to non-pharmaceutical mitigation and suppression scenarios, International Journal of Epidemiology 49 (2020) 1443-1453. https://doi.org/10.1093/ije/dyaa121.

[5] J. S. Weitz, S. J. Beckett, A. R. Coenen, D. Demory, M. Dominguez-Mirazo, J. Dushoff, C.-Y. Leung, G. Li, A. Măgălie, S. W. Park, Modeling shield immunity to reduce COVID-19 epidemic spread, Nature Medicine 26 (2020) 849-854. https://doi.org/10.1038/s41591-020-0895-3.

[6] O. Abu-Hammad, H. Alduraidi, S. Abu-Hammad, A. Alnazzawi, H. Babkair, A. Abu-Hammad, I. Nourwali, F. Qasem, N. Dar-Odeh, Side Effects Reported by Jordanian Healthcare Workers Who Received COVID-19 Vaccines, Vaccines 9 (2021) 577. https://doi.org/10.3390/vaccines9060577.

[7] R. V. Barnabas, A. Wald, A public health covid-19 vaccination strategy to maximize the health gains for every single vaccine dose, Annals of Internal Medicine 174 (2021) 552-553. https://doi.org/10.7326/M20-8060.

[8] L. J. De Picker, M. C. Dias, M. E. Benros, B. Vai, I. Branchi, F. Benedetti, A. Borsini, J. C. Leza, H. Kärkkäinen, M. Männikkö, et al., Severe mental illness and European COVID-19 vaccination strategies, The Lancet Psychiatry 8 (2021) 356-359. https://doi.org/10.1016/S2215-0366(21)00046-8.

[9] V. M. Kumar, S. R. Pandi-Perumal, I. Trakht, S. P. Thyagarajan, Strategy for COVID-19 vaccination in India: the country with thesecond highest population and number of cases, npj Vaccines 6 (2021) 60. https://doi.org/10.1038/s41541-021-00327-2.

[10] F. Casella, Can the COVID-19 epidemic be controlled on the basis of daily test reports?, IEEE Control Systems Letters 5 (2021) 1079-1084. https://doi.org/10.1109/LCSYS.2020.3009912.

[11] G. Rohith, K. B. Devika, Dynamics and control of COVID-19 pandemic with nonlinear incidence rates, Nonlinear Dynamics 101 (2020) 2013-2026. https://doi.org/10.1007/s11071-020-05774-5.

[12] M. A. Hadi, H. I. Ali, Control of COVID-19 system using a novel nonlinear robust control algorithm, Biomedical Signal Processing and Control 64 (2021) 102317. https://doi.org/10.1016/j.bspc.2020.102317.

[13] J. Köhler, L. Schwenkel, A. Koch, J. Berberich, P. Pauli, F. Allgöwer, Robust and optimal predictive control of the COVID-19 outbreak, Annual Reviews in Control 51 (2021) 525-539. https://doi.org/10.1016/j.arcontrol.2020.11.002

[14] A. Rajaei, M. Raeiszadeh, V. Azimi, M. Sharifi, State estimation-based control of COVID-19 epidemic before and after vaccine development, Journal of Process Control 102 (2021) 1-14. https://doi.org/10.1016/j.jprocont.2021.03.008.

[15] C. Boqiang, K. Ting, Nonlinear adaptive control of COVID-19 with media campaigns and treatment, Biochemical and Biophysical Research Communications 555 (2021) 202-209. https://doi.org/10.1016/j.bbrc.2020.12.105.

[16] I. Cooper, A. Mondal, C. G. Antonopoulos, A SIR model assumption for the spread of COVID-19 in different communities, Chaos, Solitons & Fractals 139 (2020) 110057. https://doi.org/10.1016/j.chaos.2020.110057.

[17] F. Colavita, F. Vairo, S. Meschi, M. B. Valli, E. Lalle, C. Castilletti, D. Fusco, G. Spiga, P. Bartoletti, S. Ursino, et al., COVID-19 Rapid Antigen Test as Screening Strategy at Points of Entry: Experience in Lazio Region, Central Italy, August–October 2020, Biomolecules 11 (2021) 425. https://doi.org/10.3390/biom11030425.

[18] A. H. Mhmood, H. I. Ali, Optimal H-infinity Integral Dynamic State Feedback Model Reference Controller Design for Nonlinear Systems, Arabian Journal for Science and Engineering 2021. https://doi.org/10.1007/s13369-021-05447-4.

[19] A. H. Mhmood, H. I. Ali, Optimal adaptive guaranteed-cost H-infinity model reference controller design for nonlinear systems, International Journal of Dynamics and Control 2021. https://doi.org/10.1007/s40435-021-00846-9.

[20] H. I. Ali, A. H. Mhmood, Nonlinear H-Infinity Model Reference Controller Design, International Review of Automatic Control (IREACO) 14 (2021) 39-50. https://doi.org/10.15866/ireaco.v14i1.20301.

[21] H. I. Ali, H-infinity Model Reference Controller Design for Magnetic Levitation System, Engineering and Technology Journal 36 (2018) 17-26. https://doi.org/10.30684/etj.36.1A.3.

[22] Z. Xu, B. Wu, U. Topcu, Control strategies for COVID-19 epidemic with vaccination, shield immunity and quarantine: A metric temporal logic approach, PloS ONE 16 (2021) e0247660. https://doi.org/10.1371/journal.pone.0247660

[23] Easy Milano, The vaccine campaign has begun in Lombardy, 2021 (accessed 9 December 2021), https://easymilano.com/living-in-italy-can-i-get-a-covid-19-vaccination/.

[24] C. R. MacIntyre, V. Costantino, M. Trent, Modelling of COVID-19 vaccination strategies and herd immunity, in scenarios of limited and full vaccine supply in NSW, Australia, Vaccine (2021). https://doi.org/10.1016/j.vaccine.2021.04.042.